Flight Testing Small UAVs for Performance Estimation

Adam T. Chase[*] and Second B. Author[*]
California Polytechnic State University, San Luis Obispo, California 93407
Business or Academic Affiliation, City, Province, Zipcode, Country

This is a bare-bones LaTeX template of an AIAA technical conference paper. It is intended to demonstrate the bare minimum set of LaTeX commands to produce an AIAA technical conference paper. To explore more LaTeX capabilities, see the advanced example, but first read the Known Problems section of the user manual. For detailed AIAA layout and style guidelines, please refer to the AIAA author guide for paper submission, format, and other procedures.

Nomenclature

J	Jacobian Matrix
f	Residual value vector
x	Variable value vector
F	Force, N
m	Mass, kg
Δx	Variable displacement vector
α	Acceleration, m/s^2

Subscript

i	Variable number

I. Introduction

An accurate drag prediction is critical for conceptual aircraft design, aircraft mission planning, and predicting performance trends of comparable aircraft. To this end, industry spends an extensive amount of time and money developing wind tunnel models and executing wind tunnel tests. Additionally, it is difficult to impossible to exactly scale down a vehicle, especially when features such as rivets, servo control horns, antennas, and air data probes are included. These differences between the model and the as-built aircraft can cause accuracy of the wind tunnel test to suffer. This inaccuracy inevitably leads to aerodynamic flight tests that attempt to quantify the as-built drag and lift characteristics of the vehicle.

The flight test of full scale aircraft for drag polar prediction is generally conducted about a trimmed condition. That is, the aircraft is flown to an operating conditions dictated by the test plan, and sets the control surfaces such that there are no accelerations and no moments. Data is then collected for a set amount of time, without changing the operating condition. After the data is collected, the operating point is changed, the aircraft is trimmed at this new flight condition, and data is again collected. This process is repeated at various points in the aircraft's flight envelope until enough data is collected to estimate a drag polar.

Unfortunately, for many R/C aircraft and small UAVs, this procedure isn't feasible. First, these aircraft typically operate close to ground level, meaning there could potentially be both unsteady and turbulent winds, and a steady wind. R/C aircraft and small UAVs typically have much lower moments of inertias and mass than their full-scale counterparts, which means they will be affected much more by atmospheric disturbances than full-scale vehicles. Second, many of these aircraft have a line-of-sight communication link,

[*]Graduate Student, Aerospace Engineering, One Grand Avenue, Student AIAA Member.

and R/C aircraft in particular are flown in small patterns at a flight field. Even in the case of a steady atmosphere, R/C aircraft usually are not well trimmed, because by the time the pilot can see if the vehicle is trimmed, he has to turn around in the pattern. This thesis attempts to fix these problems, by allowing the pilot to fly in a more generic flight path, and not relying on a still atmosphere assumption.

A. Background

This background section is here only to demonstrate `\subsection` usage. And following this, the next section level will need to be demonstrated.

1. Model

II. Simulation

A 6-DOF flight simulator was used to validated the drag prediction method before hardware was purchased. The main utility of the simulator was to provide simulated flight test data with signals that contained no noise. The actual sensors during a flight test will be noisy signals, and Guassian white noise can be added to the clean signals to check the method's sensitivity to sensor noise.

A. Simulation Environment

The flight simulator used was a model of the de Haviland Beaver that comes as a demo in Aerospace Toolbox of Simulink. The model is connected The model was modified to output required signals to the workspace, which essentially created a sensor with zero noise. The mass, moments of inertia, and reference lengths were then scaled to those of a Zagi R/C aircraft found in.[?] The original Simulink model was already connected to a Flight Gear visualization engine, but the model was altered such that the indicators would function properly.

B. Simulation Inputs

The engine forces and moments were set to zero in the simulator, to match the assumption of a folding propeller. The force calculations built into the Beaver Simulink model were replaced with a parabolic drag polar of the form $\mathrm{C}_D = C_{D_0} + K * (C_L(\alpha) - C_{L_{min}})$

The lift coefficient $C_L(\alpha)$ was nonlinear aerodynamic data from a NACA 0012 taken from.[?] While this approximation to a nonlinear drag polar does not capture the drag rise due to stall, it does represent the limited lifting capability of a real wing, making it more realistic than assuming the wing does not stall.

C. Simulation Results

The most first result of the simulation testing was a verification of the correct equations of motion. The simulation was initialized with various initial states to ensure there was no dependence on initial conditions. The vehicle was then flown by an R/C aircraft pilot using a joystick attached the to simulation. It was noted early in the simulation testing that flying a sweep of speeds was beneficial, as a wider range of the drag polar was flown. This result was included in much of the flight test planning.

One of the main goals of the simulation was to verify the data analysis routines developed in Matlab did in fact match inputs to outputs. To do this, the simulation was flown and, when finished, no noise was added to the data. The results are shown in Figure **??**.

Figure **??** shows that the equations of motion used in the data analysis functions properly calculate the coefficients being passed into the system. With this result, noise was added to the system to see how sensitive coefficient estimation was to noise in each sensor. This process was a balancing act between available sensor accuracy and accuracy of the final solution. The final result guided sensor selection to those discussed in Section **??**. To check if the final sensors chosen were acceptable, Gaussian noise was added to each state, with a mean of 0 and a standard deviation equal to the root-mean-squared error listed in the manufacturer's data sheet for each sensor.

Figure 1. Equations of Motion Verification (No Noise)

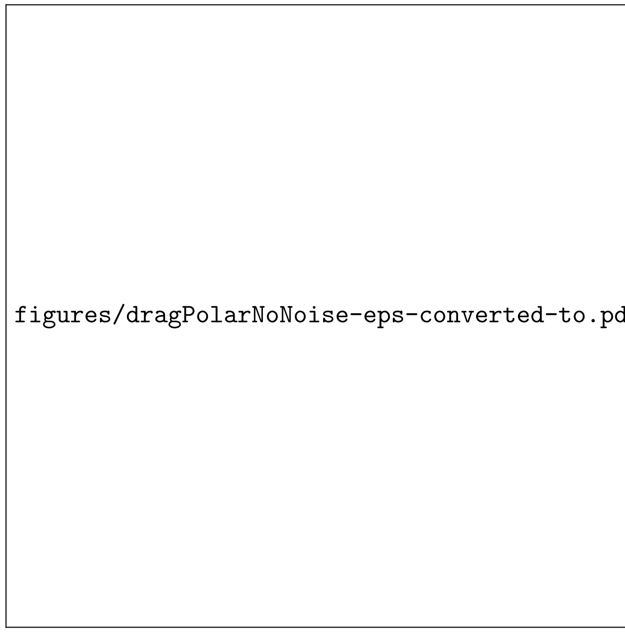

III. Results

In this section we will introduce some figures and tables. It can be seen in figure 1 that magnetization is a function of applied field. Sometimes writing meaningless text can be quiet easy, but other times one is hard pressed to keep the words flowing.[a] Meanwhile back in the other world, table 1 shows a nifty comparison.

Table 1. Variable and Fixed Coefficient Runge-Kutta Schemes as a Function of Reynolds Number

Re	Vary	Fixed
1	868	4,271
10	422	2,736
25	252	1,374
50	151	736
100	110	387
500	85	136
1,000	77	117
5,000	81	98
10,000	82	99

IV. Conclusion

After much typing, the paper can now conclude. Four rocks were next to the channel. This caused a few standing waves during the rip that one could ride on the way in or jump on the way out.

Appendix

An appendix, if needed, should appear before the acknowledgments. Use the 'starred' version of the `\section` commands to avoid section numbering.

[a]And sometimes things get carried away in endless detail.

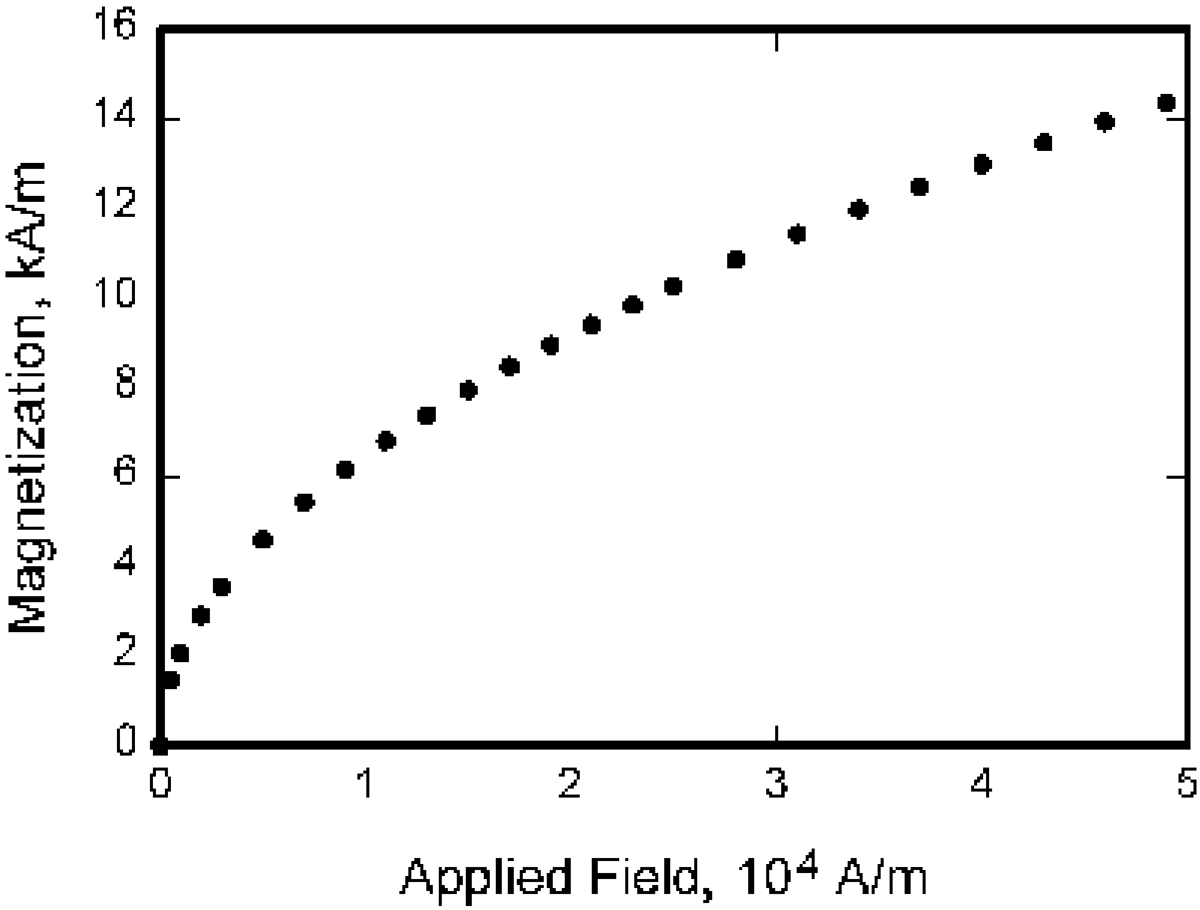

Figure 2. Magnetization as a function of applied field, which has borders so thick that they overwhelm the data and for some reason the ordinate label is rotated 90 degrees to make it difficult to read. This figure also demonstrates the dangers of using a bitmap as opposed to a vector image.

Acknowledgments

A place to recognize others.

References

[1]Rebek, A., *Fickle Rocks*, Fink Publishing, Chesapeake, 1982.